Materials Science in Semiconductor Processing 176 (2024) 108331

Contents lists available at ScienceDirect

Materials Science in Semiconductor Processing

journal homepage: www.elsevier.com/locate/mssp

Recovery at room temperature annealing on 4H–SiC SBDs by gamma irradiation

Yun Li [a,b], Min Gong [a,b], Mingmin Huang [a,b], Yao Ma [a,b], Zhimei Yang [a,b,*]

[a] *Key Laboratory for Microelectronics, College of Physics, Sichuan University, Chengdu, 610064, China*

[b] *Key Laboratory of Radiation Physics and Technology of Ministry of Education, Sichuan University, Chengdu, 610064, China*

ARTICLE INFO

Keywords:
4H–SiC
Degradation
Gamma irradiation
Schottky barrier height
Deep level defect

ABSTRACT

The impact of gamma irradiation and subsequent recovery at room temperature on the device performance of commercial 4H–SiC Schottky barrier diodes (SBDs) was investigated through the analysis of the electrical properties and the deep level transient spectroscopy (DLTS). The ideality factor (n) of the SBDs increased from 1.01 to 1.13 with an increasing irradiation dose, but recovered after 7 days of room temperature annealing. To determine Schottky barrier heights (Φ_B), both current-voltage (I–V) and capacitance-voltage (*C*–V) measurements were performed. The results of the combined I–V and *C*–V analysis showed that a little variations in Φ_B were consistent with the variations in irradiation dose, except for the Φ_B calculated by *C*–V measurement at 30 kGy. Similarly, the Φ_B recovered after 7 days at room temperature. DLTS analysis revealed the presence of Z_1/Z_2 traps in the samples after 7 days at room temperature annealing. These traps exhibited activation energies ranging from 0.46 eV to 0.55 eV. The trap concentration (N_T) increased from 9.48×10^{12} cm^{-3} to 2.23×10^{13} cm^{-3} with the increasing irradiation dose. These findings indicate that gamma irradiation-induced point defects were the primary cause of the degradation of 4H–SiC SBDs.

1. Introduction

With the continuous development of the aerospace industry, the radiation hardness of semiconductor devices has become a crucial requirement. 4H–SiC is a highly promising semiconductor material for high temperature and harsh radiation environments due to its high critical displacement energy, high mobility, and high thermal conductivity [1–3]. However, the reliability of these devices under high-energy radiation, particularly gamma rays, remains a critical concern. The use of γ-ray emitted by a^{60}Co source is widely employed to investigate the ionizing radiation damage in semiconductor devices [4–9]. These γ-rays generate secondary electrons that induce the displacement damage in SiC, leading to the introduction of carrier traps and recombination centers [10]. While, according to D.C. Sheridan [11] the reverse leakage current were unaffected by the high dose γ-ray irradiation. Similar, other publications have observed little significant degradation in SiC devices following γ-ray irradiation [12,13]. But, some studies have reported a decrease in leakage current density in 4H/6H–SiC after γ-ray irradiation due to the reduction in the tunneling current [14] or the effect of the point defects caused by the γ-ray irradiation [15]. In contrast to the above some researchers have observed that an increase in the reverse leakage currents because of the consequence of ionization damage [16]. However, studies have shown that SiCis relatively insensitive to the ionization process [17,18], with only a few point defects being produced under swift heavy ion irradiation conditions. Despite the extensive research conducted on the radiation effects on SiC-based devices in recent decades [19,20], the degradation mechanism under γ-ray irradiation remains unclear. Moreover, only a small portion of the research has focused specifically on gamma irradiation effects on SiC devices. Therefore, there is still a need to clarify the degradation mechanism of the SiC under γ-ray irradiation through comprehensive experimental studies.

Among various SiC power devices, 4H–SiC Schottky Barrier diode (SBD) is a relatively mature SiC power device with low on-resistance, high avalanche breakdown electric field, short reverse recovery time, and good high-temperature characteristics [21,22]. It is widely used in the commercial field. In the present work, commercially available 4H–SiC SBDs were subjected to ^{60}Co γ-ray doses up to 30 kGy, and their electrical characteristics were analyzed using current-voltage (I–V) and capacitance-voltage (*C*–V). Furthermore, the deep level transient spectroscopy (DLTS) was employed to characterize the parameters of the traps present in the irradiated samples. Additionally, the changes in the

* Corresponding author. Key Laboratory for Microelectronics, College of Physics, Sichuan University, Chengdu, 610064, China.
E-mail address: yangzhimei@scu.edu.cn (Z. Yang).

https://doi.org/10.1016/j.mssp.2024.108331
Received 22 December 2023; Received in revised form 24 February 2024; Accepted 11 March 2024
Available online 14 March 2024
1369-8001/

electrical characteristics of γ-irradiated samples were investigated after 7 days at room temperature. This research aims to provide more detailed insights and clues about the degradation mechanism of SiC SBD under γ-ray irradiation.

2. Experimental procedure

This experiment utilized SCS106AG SiC SBDs manufactured by ROHM Company. The rectifier SCS106AG SiC SBDs are a typical package TO-220AC and commonly employed in switch mode power supplies, power factor correction, and motor drives.

2.1. Details of γ-ray irradiation

The γ-ray irradiation experiments were performed at the Institute of Biotechnology and Nuclear Technology, Sichuan Academy of Agricultural Sciences. The samples were irradiated with γ-rays emitted by ^{60}Co radiation sources in the horizontal direction with 1.25 MeV at room temperature under zero bias voltage conditions. The dose rate was 1.38 Gy(Si)/s. Four independent experiments were performed using a ^{60}Co γ source with doses of 5 kGy, 7.5 kGy, 10 kGy, and 30 kGy. After γ-ray irradiation, all the irradiated samples were stored in dry ice after to prevent annealing at room temperature. The first measurements were conducted within 24 h following γ-ray irradiation. Subsequently, to observe the effect of room temperature annealing on the SiC SBDs device performance, the samples were kept at room temperature for 7 days before the second measurement, while maintaining the same test parameters.

2.2. I–V and C–V measurements

The current-voltage (I–V) and the capacitance-voltage (*C*–V) measurements were carried using the Agilent B2902A Semiconductor Device Analyzer at room temperature. The I–V measurement involved applying a bias voltage ranging from −40 V to 5 V, while the *C*–V measurement used a bias voltage range from −25 V to 1 V.

2.3. Deep level transient spectroscopy (DLTS) measurements

To calculate the parameters of the deep level defects induced by γ irradiation (such as capture-cross section, trap concentration, and other parameters), the PHYSTECH FT-1230 HEAR deep level transient spectroscopy (DLTS) was utilized. The temperature of the device was controlled using the CRYO.CON 22C Temperature Controller, EDWARDS T-Station85 molecular pump, and CTI-CRYOGENICS compressor, ensuring a vacuum environment. DLTS measurements were performed by scanning temperatures from 40 K to 500 K. The measurement conditions were set as $U_P = -0.2$ V, $U_R = -6$ V, $T_W = 0.1$ ms and $t_P = 10^{-4}$ ms, where U_P is the voltage of fill pulse, U_R is the reverse bias, T_W is the period width and t_P is the filling pulse width.

3. Experimental results and discussion

Fig. 1 displays the forward and reverse I–V characteristics of post-irradiation SiC SBD and after 7 days. It can be seen from Fig. 1 that the forward currents of all the samples changed slightly, including the series resistance. The SiC SBD with the highest irradiation dose (30 kGy) exhibited the highest forward current. Additionally, the forward currents showed little change at room temperature after 7 days compared to their initial values. The leakage current increased compared to the non-irradiated device, particularly under larger reverse bias. According to the following equations (1) and (2), the current density generated in the potential barrier region (J_G) is higher than the reverse current diffusion density (J_{RD}) due to the smaller intrinsic carrier concentration (n_i) in wide band gap SiC device. The width of the potential energy barrier (X_D) increases with the reverse bias voltage, resulting in unsaturated current

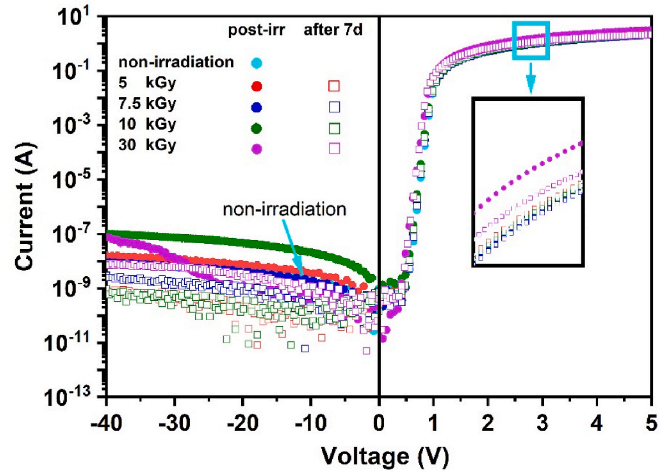

Fig. 1. Forward and reverse I–V characteristics under different doses post-irradiation and after 7 days under room temperature.

in the potential barrier region that gradually increases with the reverse bias voltage.

$$J_G = \frac{qn_iX_D}{2\tau} \tag{1}$$

$$J_{RD} = \frac{qD_Pn_i^2}{L_P\,N_D} \tag{2}$$

where q is the charge of the electron, τ is the non-equilibrium charge carrier lifetime, D_P is the hole diffusion coefficient, L_P is the diffusion length of non-equilibrium charge carrier, N_D is the doping concentration.

However, after 7 days at room temperature, the leakage current decreased compared to the immediate post-irradiation state and even became smaller than the non-irradiated condition. Therefore, the increase in the leakage current of SiC SBDs implies that the introduction of defects by γ-ray irradiation, with these irradiation-induced defects showing recovery after 7 days at room temperature. The increase in the leakage irradiated SiC SBDs was attributed to the ionization damage induced by γ-rays irradiation [23]. In fact, γ irradiation can also introduce point defects [15] and even displacement damage to SiC [10], with the point defect contributing to the increased leakage current. Thus, the current variation caused by γ irradiation is influenced by multiple factors, which can lead to either an increase or decrease in current. However, those results indicate that γ irradiation annealing at room temperature can effectively improve the leakage current of the device.

According to the thermionic emission (TE) theory, the relationship between the forward current and the forward bias voltage can be explained by the following equation (3) and (4) [24], which does not consider the series resistance:

$$I = I_s\left[\exp\left(\frac{qV}{nkT}\right) - 1\right] \tag{3}$$

where,

$$I_s = A^*AT^2\exp\left(-\frac{q\Phi_B}{kT}\right) \tag{4}$$

I_s is the reverse saturation current, A* is the effective Richardson constant (146 A cm^{-2}K^{-2} for 4H–SiC) [25], A is the effective area of the diode (approximately equal to 1.46 mm^2), T is the absolute temperature, Φ_B is the Schottky barrier height, k is the Boltzmann constant, V is the applied voltage, and n is the ideality factor.

When V > 3kT/q, the I_s can be neglected. The n and Φ_B can be obtained from formula (5) and (6) respectively. They can be expressed as:

$$n = \frac{q}{kT}\frac{\mathrm{d}V}{\mathrm{d}(\ln I)} \tag{5}$$

$$\Phi_B = \frac{kT}{q}\ln\left(\frac{A^{*}AT^{2}}{I_S}\right) \tag{6}$$

The values of n and Φ_B with the dose change are shown in Fig. 2. The n increased from 1.01 at non-irradiation to 1.13 at 30 kGy. After 7 days of room temperature annealing, the overall decrease in n was observed, with the value at 30 kGy decreasing from 1.13 to 1.11. The Φ_B of all irradiated samples exhibited little change compared to the non-irradiated samples. After 7 days of room temperature annealing, there was a slight overall increase in Φ_B.

Furthermore, the *C*–V characteristics of all devices were measured at room temperature with a frequency of 1 MHz. The $1/C^2$–V plots of samples are shown in Fig. 3. It is noted that the change in capacitance was more pronounced with increasing irradiation dose, particularly for the 30 kGy sample.

The Φ_B and N_D of SiC SBD can be extracted from the $1/C^2$–V plots using the standard equation (7) [26]:

$$\frac{1}{C^2} = \frac{2}{q\varepsilon_S\varepsilon_0 N_D A^2}(V_i - V_R) \tag{7}$$

and the Φ_B is given by equation (8):

$$\Phi_B = V_{bi} + V_n = V_i + \frac{kT}{q} + \frac{kT}{q}\ln\left(\frac{N_C}{N_D}\right) \tag{8}$$

where ε_S is the static dielectric constant of 4H–SiC (equal to 9.7) [27], ε_0 is the permittivity of free space, V_i is the diffusion potential and estimated by extrapolating the $1/C^2$–V plots on the voltage axis, V_R is the reverse voltage, V_{bi} is the built-in voltage, N_C is effective charge carrier density of states in the conduction band and equal to 1.69×10^{19} cm^{-3} for 4H–SiC.

The values of N_D and the Φ_B obtained from the *C*–V measurement are shown in Fig. 4. With an increase in the irradiation dose, the N_D showed a slightly increase, but significantly decreased at a dose of 30 kGy. However, following 7 days of room temperature annealing, the N_D showed a slight increase with minimal change, especially at 30 kGy. The trend of Φ_B change calculated by *C*–V measurement was different significantly from that of I–V measurement at a dose of 30 kGy.

Table 1 presents a comparison between the Φ_B values derived from the I–V and *C*–V measurements. It can be found that the Φ_B values obtained from the *C*–V measurements were significantly higher than those obtained from the I–V measurements. The difference between the $\Phi_{B(I-V)}$ and the $\Phi_{B(C-V)}$ may be attributed to several factors, including the presence of a thin layer at the interface between the metal and semiconductor, the inhomogeneous Schottky contacts, the substrate misorientation, and the non-uniformity doping [28]. The I–V characteristic is highly dependent on the interface homogeneity, while the value of $\Phi_{B(C-V)}$ approaches the flat-band Φ_B is less affected by the interface homogeneity [29,30]. Additionally, the interfacial defects can increase the V_{bi}, leading to an increase in the $\Phi_{B(C-V)}$ [31]. Furthermore, an increase in the N_D extracted from the *C*–V measurement results in an increase in the Fermi level (E_F) on the semiconductor, leading to a decrease in the

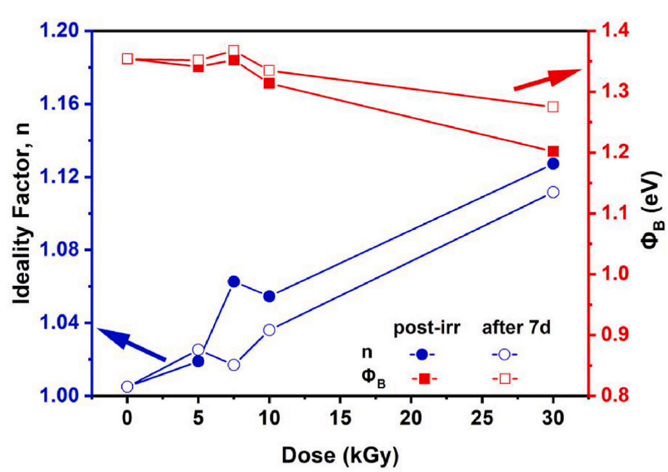

Fig. 2. Extracted n and Φ_B versus γ-ray irradiation dose post-irradiation and after 7 days of room temperature annealing from I–V measurements.

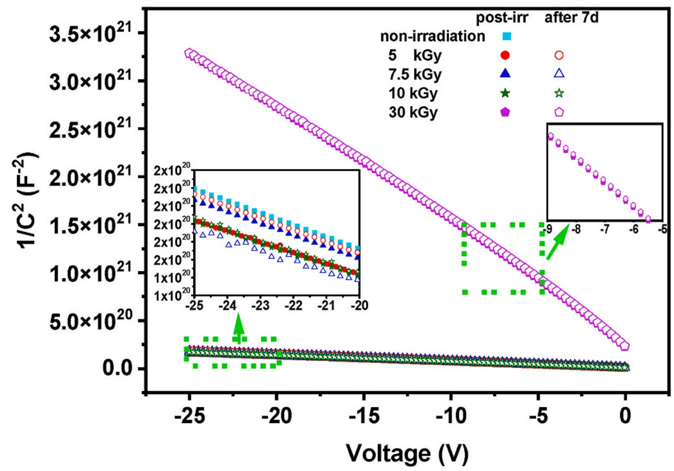

Fig. 3. The $1/C^2$–V plots of all devices at different doses post-irradiation and after 7 days of room temperature annealing.

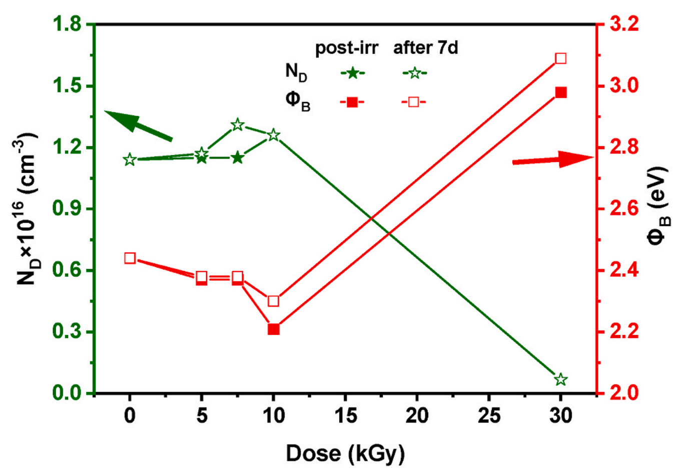

Fig. 4. The N_D and Φ_B versus γ-ray irradiation dose post-irradiation and after 7 days of room temperature annealing from *C*–V measurements.

Table 1
The comparison of Φ_B values derived from I–V and *C*–V measurement.

Dose (kGy) & Annealing state	Measurement technique of Φ_B (eV)		N_D (cm^{-3})	n
	I–V $\Phi_{B(I-V)}$	*C*–V $\Phi_{B(C-V)}$		
Non-irradiation	1.35	2.44	1.14×10^{16}	1.01
5	1.34	2.37	1.15×10^{16}	1.02
5 after 7 days	1.35	2.38	1.17×10^{16}	1.03
7.5	1.35	2.37	1.15×10^{16}	1.06
7.5 after 7 days	1.37	2.38	1.31×10^{16}	1.02
10	1.31	2.21	1.26×10^{16}	1.05
10 after 7 days	1.33	2.30	1.26×10^{16}	1.04
30	1.20	2.98	6.71×10^{14}	1.13
30 after 7 days	1.27	3.09	6.72×10^{14}	1.11

work function on semiconductor (W_S). Consequently, a higher N_D corresponds to a lower Φ_B. The most obvious result was that a significant decrease in N_D at a dose of 30 kGy led to a significant increase in Φ_B as shown in Fig. 4 and Table 1. $\Phi_{B(I-V)}$ is related to interface homogeneity, while $\Phi_{B(C-V)}$ is related to flat-band Φ_B which is affected by N_D. This indicated that defects and interfacial states could be significantly induced in SiC SBD devices at higher doses of γ-rays radiation, leading to an increase in the Φ_B extracted from $1/C^2$–V. According to equation (8), $\Phi_{B(C-V)}$ is mainly determined by V_i and N_D. Therefore, there were some small differences in $\Phi_{B(C-V)}$ under the same N_D. All Φ_B increased after 7 days of room temperature annealing. The inhomogeneity of the Schottky barrier height distribution results in the difference between the $\Phi_{B(I-V)}$ and the $\Phi_{B(C-V)}$. Previous studies have described the inhomogeneity of Φ_B using a modified TE model with Gaussian distribution [28]. The $\Phi_{B(I-V)}$ is close to the lowest barrier height, while the $\Phi_{B(C-V)}$ is close to the highest barrier height [28].

DLTS measurements were performed to identify the defects causing the Φ_B change and obtain insight into the nature of these defects. In fact, as the DLTS test is performed up to 500 K, it will cause the high-temperature annealing caused by the DLTS measurement, which limits the distinction of deep level defects introduced after γ-ray irradiation. Nevertheless, DLTS measurements of samples after 7 days of room temperature annealing provide some understanding the effect of defects on the Φ_B and the degradation mechanism. The DLTS spectra showed a single dominant peak at around 325 K for all devices (Fig. 5).

The thermal activation energy and the apparent capture cross section (σ) can be calculated from the Arrhenius plot that reflects the temperature dependence of the thermal emission rates [32]. The trap concentration (N_T) can be determined by the peak height in the DLTS spectrum [33]. Table 2 presents the DLTS parameters, indicating a correlation between the changes in the N_T and the amplitude of the DLTS peak, as the peak of DLTS amplitude is proportional to the defect concentration. The activation energy of all samples ranges from 0.46 eV to 0.55 eV, indicating the presence of Z_1/Z_2 centers [34–36]. These centers are stable defects in 4H–SiC [37] and have an impact on the minority carrier life in n-type 4H–SiC materials [38,39]. While annealing at temperatures between 1500 °C and 1700 °C can reduce Z_1/Z_2 centers and increase the minority carrier lifetime when the annealing temperature is up to 1600 °C [40]. L. Storasta et al. also reported that the Z_1/Z_2 center could be eliminated by annealing above 1600 °C [41]. Thus, the Z_1/Z_2 centers cannot be eliminated by annealing at room temperature for 7 days, and their presence is likely related to the intrinsic point defects, likely involving carbon vacancy (V_C) or carbon interstitial (C_i). The σ and the N_T increased with the irradiation dose, indicating an increasing the number of carbon-related defects. Although γ irradiation did not seem to introduce new types of defects, it led to an increase in Z_1/Z_2 center concentration. The inhomogeneity of the Schottky barrier height, the localized extreme energy pulses, and the lattice damage are the three main reasons for the degradation [42]. Therefore, combining the analysis of electrical properties and DLTS tests above, the degradation mechanism of 4H–SiC SBDs in this experiment primarily resulted from γ irradiation-induced point defects, which acted as recombination centers leading to an increase in n.

4. Conclusion

In summary, the effects of γ irradiation and annealing on commercial 4H–SiC SBDs were investigated using I–V, *C*–V, and DLTS measurements. Experiment results demonstrated that as the γ irradiation dose increased, there was an increase in n, followed by a partial recovery after 7 days annealing at room temperature. γ irradiation might induce defects, affecting N_D and $\Phi_{B(C-V)}$, respectively. The stable Z_1/Z_2 traps were observed, with an increase in the N_T of the Z_1/Z_2 traps corresponding to the γ irradiation dose. Based on these findings, it can be concluded that the degradation mechanism of 4H–SiC SBDs in this work was primarily attributed to the introduction of point defects caused by γ irradiation.

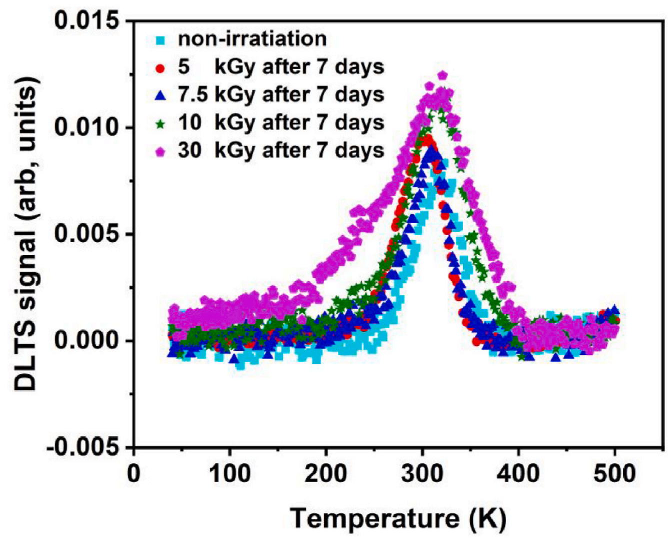

Fig. 5. Standard DLTS spectra for different doses after 7 days of room temperature annealing.

Table 2
The DLTS parameters of 4H–SiC SBD devices by γ-ray irradiated after7 days of room temperature annealing.

Dose (kGy)	E_T (eV)	σ (cm^2)	N_T (cm^{-3})
Non-irradiation	E_C-0.46	3.12×10^{-18}	9.48×10^{12}
5	E_C-0.53	1.65×10^{-17}	1.10×10^{13}
7.5	E_C-0.50	5.19×10^{-15}	9.24×10^{12}
10	E_C-0.55	1.37×10^{-15}	1.43×10^{13}
30	E_C-0.54	7.18×10^{-15}	2.23×10^{13}

CRediT authorship contribution statement

Yun Li: Writing – review & editing, Writing – original draft, Formal analysis, Data curation. **Min Gong:** Investigation, Funding acquisition. **Mingmin Huang:** Supervision, Resources, Formal analysis. **Yao Ma:** Investigation. **Zhimei Yang:** Writing – review & editing, Supervision, Resources, Conceptualization.

Declaration of competing interest

The authors declare that they have no known competing financial interests or personal relationships that could have appeared to influence the work reported in this paper.

Data availability

Data will be made available on request.

Acknowledgments

This work was supported by the National Natural Science Foundation of China under Grant No. 61974096, Natural ScienceFoundation of Sichuan Province under Grant No.2022NSFSC0874.

References

[1] J.L. Hudgins, Wide and narrow bandgap semiconductors for power electronics: a new valuation, J. Electron. Mater. 32 (6) (2003) 471–477, https://doi.org/10.1007/s11664-003-0128-9.
[2] R. Singh, Reliability and performance limitations in SiC power devices, Microelectron. Reliab. 46 (5–6) (2006) 713–730, https://doi.org/10.1016/j.microrel.2005.10.013.
[3] E. Omotoso, W.E. Meyer, S.M.M. Coelho, M. Diale, P.N.M. Ngoepe, F.D. Auret, Electrical characterization of defects introduced during electron beam deposition

of W Schottky contacts on n-type 4H-SiC, Mater. Sci. Semicond. Process. 51 (2016) 20–24, https://doi.org/10.1016/j.mssp.2016.04.012.
[4] J. Li, C. Chiang, X. Xia, S. Stepanoff, A. Haque, D.E. Wolfe, F. Ren, S.J. Pearton, Reversible total ionizing dose effects in NiO/Ga_2O_3 heterojunction rectifiers, J. Appl. Phys. 133 (2023) 015702, https://doi.org/10.1063/5.0134823.
[5] R. Chen, Y. Liang, J. Han, Q. Lu, Q. Chen, Z. Wang, H. Wang, X. Wang, R. Yuan, Research on the synergistic effect of total ionization and displacement dose in GaN HEMT using neutron and gamma-ray irradiation, Nanomaterials 12 (13) (2022) 2126, https://doi.org/10.3390/nano12132126.
[6] Y. Sun, X. Wan, Z. Liu, H. Jin, J. Yan, X. Li, Y. Shi, Investigation of total ionizing dose effect in 4H–SiC power MOSFET under gamma ray radiation, Radiat. Phys. Chem. 197 (2022) 110219, https://doi.org/10.1016/j.radphyschem.2022.110219.
[7] J. Shi, X. Wang, X. Zhang, J. Xue, X. Guo, M. Li, J. Wang, X. Meng, B. Cui, X. Yu, L. Yu, W. Jiang, S. Peng, Synergistic effects in MOS capacitors with an Au/HfO_2–SiO_2/Si structure irradiated with neutron and gamma ray, J. Phys. Appl. Phys. 55 (2022) 115104, https://doi.org/10.1088/1361-6463/ac3ce8.
[8] H.Y. Zahran, E.S. Yousef, I.S. Yahia, Novel approach of gamma attenuation performance of $Cu_2SnZn(S,Se,Te)_4$ semiconductor materials: radiation interactions with proton, alpha, carbon, electron, and photon, Mater. Sci. Semicond. Process. 123 (2021) 105554, https://doi.org/10.1016/j.mssp.2020.105554.
[9] S.M. Ali, M.S. AlGarawi, S.U. Khan, S. Aldawood, Nanostructure, optical and electrical response of gamma ray radiated PdS/p-Si heterojunction, Mater. Sci. Semicond. Process. 122 (2021) 105474, https://doi.org/10.1016/j.mssp.2020.105474.
[10] S. Onoda, T. Ohshima, T. Hirao, K. Mishima, S. Hishiki, N. Iwamoto, K. Kojima, K. Kawano, Decrease of charge collection due to displacement damage by gamma rays in a 6H-SiC diode, IEEE Trans. Nucl. Sci. 54 (6) (2007) 1953–1960, https://doi.org/10.1109/TNS.2007.910203.
[11] D.C. Sheridan, G. Chung, S. Clark, J.D. Cressler, The effects of high-dose gamma irradiation on high-voltage 4H-SiC Schottky diodes and the SiC-SiO_2 interface, IEEE Trans. Nucl. Sci. 48 (6) (2001) 2229–2232, https://doi.org/10.1109/23.983200.
[12] I.P. Vali, P.K. Shetty, M.G. Mahesha, V.C. Petwal, Jishnu Dwivedi, D.M. Phase, R. J. Choudhary, Electron and gamma irradiation effects on Al/n−4H–SiC Schottky contacts, Vacuum (172) (2020) 109068, https://doi.org/10.1016/j.vacuum.2019.109068.
[13] Z. Li, J. Wu, K. Wu, Y. Fan, Z. Bai, Y. Jiang, Y. Yin, Q. Xie, J. Lei, The performance of 4H–SiC detector at high temperature after gamma irradiation, Radiat. Phys. Chem. 162 (2019) 153–156, https://doi.org/10.1016/j.radphyschem.2019.05.004.
[14] P. Vigneshwara Raja, N.V.L. Narasimha Murty, Thermally stimulated capacitance in gamma irradiated epitaxial 4H-SiC Schottky barrier diodes, Journal of Appled Physics 123 (2018) 161536, https://doi.org/10.1063/1.5003068.
[15] J.H. Ha, S.M. Kang, Y.H. Cho, S.H. Park, H.S. Kim, J.H. Lee, N.H. Lee, Y.K. Kim, J. K. Kim, Schottky barrier heights of semi-insulating 6H-SiC irradiated by high-dose γ-rays, Nucl. Instrum. Methods Phys. Res. 580 (1) (2007) 416–418, https://doi.org/10.1016/j.nima.2007.05.068.
[16] A.Y.C. Yu, E.H. Snow, Radiation effects on silicon Schottky barriers, IEEE Trans. Nucl. Sci. 16 (6) (1969) 220–226, https://doi.org/10.1109/TNS.1969.4325530.
[17] S. Sorieul, X. Kerbiriou, J.-M. Costantini, L. Gosmain, G. Calas, C. Trautmann, Optical spectroscopy study of damage induced in 4H-SiC by swift heavy ion irradiation, J. Phys. Condens. Matter 24 (12) (2012) 125801, https://doi.org/10.1088/0953-8984/24/12/125801.
[18] M. Backman, M. Toulemonde, O.H. Pakarinen, N. Juslin, F. Djurabekova, K. Nordlund, A. Debelle, W.J. Weber, Molecular dynamics simulations of swift heavy ion induced defect recovery in SiC, Comput. Mater. Sci. 67 (2013) 261–265, https://doi.org/10.1016/j.commatsci.2012.09.010.
[19] Z. Yang, Y. Ma, M. Gong, Y. Li, M. Huang, B. Gao, X. Zhao, Recrystallization effects of swift heavy ^{209}Bi ions irradiation on electrical degradation in 4H-SiC Schottky barrier diode, Nucl. Instrum. Methods Phys. Res., Sect. B 401 (2017) 51–55, https://doi.org/10.1016/j.nimb.2017.02.004.
[20] Z. Yang, F. Lan, Y. Li, M. Gong, M. Huang, B. Gao, J. Hu, Y. Ma, The effect of the interfacial states by swift heavy ion induced atomic migration in 4H-SiC Schottky barrier diodes, Nucl. Instrum. Methods Phys. Res., Sect. B 436 (2018) 244–248, https://doi.org/10.1016/j.nimb.2018.09.024.
[21] R. Madar, Silicon carbide in contention, Nature 430 (2004) 974–975, https://doi.org/10.1038/430974a.
[22] T. Kimoto, J.A. Cooper, Fundamentals of Silicon Carbide Technology: Growth, Characterization, Devices and Applications, Wiley-IEEE Press, 2014.
[23] A.Y.C. Wu, E.H. Snow, Radiation effects on silicon Schottky barriers, IEEE Trans. Nucl. Sci. 16 (6) (1969) 220–226, https://doi.org/10.1109/TNS.1969.4325530.
[24] E.H. Rhoderick, R.H. Williams, Metal−Semiconductor Contacts, second ed., Oxford Science Publication, 1988.
[25] B.J. Baliga, Silicon Carbide Power Devices, World Scientific, Singapore, 2005.
[26] Ł. Gelczuk, P. Kamyczek, E. Płaczek-Popko, M. Dąbrowska-Szata, Correlation between barrier inhomogeneities of 4H-SiC 1A/600V Schottky rectifiers and deep-level defects revealed by DLTS and Laplace DLTS, Solid State Electron. 99 (2014) 1–6, https://doi.org/10.1016/j.sse.2014.04.043.
[27] R. Singh, Reliability and performance limitations in SiC power devices, Microelectron. Reliab. 46 (2006) 713–730, https://doi.org/10.1016/j.microrel.2005.10.013.
[28] C. Raynaud, K. Isoird, M. Lazar, C.M. Johnson, N. Wright, Barrier height determination of SiC Schottky diodes by capacitance and current–voltage measurements, J. Appl. Phys. 91 (2002) 9841–9847, https://doi.org/10.1063/1.1477256.
[29] R.T. Tung, Electron transport at metal-semiconductor interfaces: general theory, Phys. Rev. B (45) (1992) 13509–13523, https://doi.org/10.1103/PhysRevB.45.13509.
[30] J.P. Sullivan, R.T. Tung, M.R. Pinto, W.R. Graham, Electron transport of inhomogeneous Schottky barriers: a numerical study, J. Appl. Phys. 70 (12) (1991) 7403–7424, https://doi.org/10.1063/1.349737.
[31] E.H. Rhoderick, R.H. Williams, Metal-semiconductor Contacts, Clarendon Press, Oxford (UK), 1988.
[32] D.V. Lang, Deep-level transient spectroscopy: a new method to characterize traps in semiconductors, J. Appl. Phys. 45 (7) (1974) 3023–3032, https://doi.org/10.1063/1.1663719.
[33] N. Shashank, Vikram Singh, Sanjeev K. Gupta, K.V. Madhu, J. Akhtar, R. Damle, DLTS and in situ C-V analysis of trap parameters in swift 50 MeV Li^{3+} ionirradiated Ni/SiO_2/Si MOS capacitors, Radiat. Eff. Defect Solid 166 (4) (2011) 313–322, https://doi.org/10.1080/10420150.2011.553954.
[34] N.T. Son, X.T. Trinh, L.S. Løvlie, B.G. Svensson, K. Kawahara, J. Suda, T. Kimoto, T. Umeda, J. Isoya, T. Makino, T. Ohshima, E. Janzén, Negative-U system of carbon vacancy in 4H-SiC, Phys. Rev. Lett. 109 (18) (2012) 187603, https://doi.org/10.1103/PhysRevLett.109.187603.
[35] T.A.G. Eberlein, R. Jones, P.R. Briddon, Z_1/Z_2 defects in 4H-SiC, Phys. Rev. Lett. 90 (22) (2003) 225502, https://doi.org/10.1103/PhysRevLett.90.225502.
[36] C.G. Hemmingsson, N.T. Son, A. Ellison, J. Zhang, E. Janzén, Negative-U centers in 4H silicon carbide, Phys. Rev. B 58 (1998) R10119–R10122, https://doi.org/10.1103/PhysRevB.58.R10119.
[37] T. Dalibor, G. Pensl, H. Matsunami, T. Kimoto, W.J. Choyke, A. Schoner, N. Nordell, Deep defect centers in silicon carbide monitored with deep level transient spectroscopy, Phys. Status Solidi 162 (1) (1997) 199–225, https://doi.org/10.1002/1521-396X(199707)162:1<199::AID-PSSA199>3.0.CO;2-0.
[38] L. Storasta, H. Tsuchida, Reduction of traps and improvement of carrier lifetime in 4H-SiC epilayers by ion implantation, Appl. Phys. Lett. 90 (2007) 062116, https://doi.org/10.1063/1.2472530.
[39] T. Hiyoshi, T. Kimoto, Reduction of deep levels and improvement of carrier lifetime in n-type 4H-SiC by thermal oxidation, APEX 2 (4) (2009) 041101, https://doi.org/10.1143/APEX.2.041101.
[40] T. Miyazawa, H. Tsuchida, Point defect reduction and carrier lifetime improvement of Si- and C-face 4H-SiC epilayers, J. Appl. Phys. 113 (8) (2013) 083714, https://doi.org/10.1063/1.4793504.
[41] L. Storasta, H. Tsuchida, T. Miyazawa, T. Ohshima, Enhanced annealing of the $Z_1/_2$ defect in 4H–SiC epilayers, J. Appl. Phys. 103 (2008) 013705, https://doi.org/10.1063/1.2829776.
[42] Z. Wu, Y. Bai, C. Yang, J. Lu, L. Yang, Y. Tang, X. Tian, X. Liu, Schottky barrier characteristic analysis on 4H-SiC Schottky barrier diodes with heavy ion-induced degradation, IEEE Trans. Nucl. Sci. 69 (4) (2022) 932–937, https://doi.org/10.1109/TNS.2022.3160181.